Marine zooplankton acclimated to geological warming while facing limits by the next century

Rui Ying[1*], Fanny M. Monteiro[2], Jamie D. Wilson[13], Daniela N. Schmidt[1]

1 School of Earth Sciences, University of Bristol, Bristol, UK
2 School of Geographical Sciences, University of Bristol, Bristol, UK
3 Department of Earth, Ocean and Ecological Sciences, University of Liverpool, Liverpool, UK

[*]Correspondence: rui.ying@bristol.ac.uk

Abstract

Climate changes have threatened marine organisms causing migrations, biomass reduction and extinctions. However, the capacity of marine species to adapt or acclimate to these changes remains poorly constrained in both geological and anthropogenic timescales. Such uncertainty makes modelling past and future ocean biodiversity and ecosystem functions challenging, particularly for the plankton community transferring energy to the whole ocean food web. Here, we use a global trait-based plankton model to estimate the thermal acclimation of planktic foraminifera (calcifying zooplankton) in the Last Glacial Maximum (LGM, 21 ka), the pre-industrial (PI) era and future (2100) under 1 to 4°C warming scenarios. The model shows that, during the slow deglacial transition (LGM to PI), the spinose (symbiont and non-symbiont) foraminifera ecogroups have acclimated while non-spinose (non-symbiont) foraminifera kept the same thermal preference. Our model result is supported by global fossil abundance datasets in the LGM and PI. Our study thus provides the first evidence that marine plankton can acclimate during the last deglacial warming, which we confirm by re-analyzing a longer-term global fossil observation (600 ka). However, with global warming continuing, our model predicts that the acclimation capacity of these ecogroups is saturating. Due to little acclimation to anthropogenic warming, foraminifera are forced to migrate poleward, dropping their global biomass by 2.5-12.2% by 2100 relative to 2022 (depending on the warming scenarios). Despite paleo-evidence of foraminifera thermal acclimation, our study suggests that the current warming is pushing marine calcifiers outside their acclimation limits, which will worsen by 2100. This vulnerability might be stronger considering ocean acidification and symbiont bleaching effects.

Main text

Geological and modern climate changes have threatened marine biodiversity and ecosystem function (*1*, *2*). To avoid extinction, marine taxa have shifted their habitat to grow in more suitable environments (*3–6*). Alternatively, some species can rapidly adjust their physiology to persist in their local environment thanks to adaptation (i.e., evolution; (*7–10*)) or acclimation (i.e., phenotypic plasticity; (*11*)), particularly in those marine plankton with short reproductive cycle. However, the exact capacity of plankton species to adapt and acclimate remains poorly constrained in both past and ongoing climate events. Lack of this knowledge might lead to overestimated plankton extinction risk (*12*, *13*), mismatched distributional shifts (*14*, *15*), and uncertain energy supply to the whole marine food web (*16*) when assessing the impacts of climate change.

Understanding adaptation and acclimation in geological time also informs marine faunal-based paleoclimatology reconstructions. Prior studies have used calcifying plankton to estimate past ocean temperatures relying on the idea that fossil assemblages have the same thermal preference as modern assemblages ("transfer function" proxies) (*17*, *18*). For instance, planktic foraminifera are one of the most studied marine calcifying zooplankton in the paleoceanography proxies and also contribute to roughly half of the modern ocean calcium carbonate production (*19*). Their niche was considered conservative during glacial-interglacial cycles (*20*, *21*). However, the limited acclimation of foraminifera appears to mismatch their extensive phenotypic plasticity observed in both modern (*22*, *23*) and past

(*24*), particularly for some warm species' optimal niche (i.e., a subset of niche where they exhibit the highest fitness) (*21*). A further examination is required to understand foraminiferal acclimation ability to geological warming and improve our understanding of past sea surface temperature.

Here we modeled the thermal performance of planktic foraminifera community in the geological, modern, and future times. We applied an Earth System Model of Intermediate Complexity (cGENIE)to (a) the Last Glacial Maximum (LGM; ~21,000 years ago, ~6°C cooler than pre-industrial era); (b) the pre-industrial (PI, 1765-1850), era; (c) and the next century (2100) under 1-4 °C warming scenarios relative to the pre-industrial age. The cGENIE Earth System Model includes a trait-based mechanistic plankton model (*25*) that incorporates the main foraminifera ecogroups (symbiont-barren non-spinose, symbiont-barren spinose and symbiont-obligate spinose foraminifera) (*26*). Each ecogroup's thermal performance is flexible and depends on the interaction between the ecogoup's set of functional traits (size, spine, symbiont) and abiotic (temperature, nutrient, light) and biotic environmental conditions (resource competition and grazing pressure from higher trophic levels) (see **Materials and Methods**). We also estimated the observed foraminifera thermal performance in the LGM and PI using fossil records of foraminifera shells and related geochemical temperature reconstruction (see **Materials and Methods**).

Plankton thermal performance changes during the last deglacial warming

From the LGM to PI, the model agrees with the fossil observations showing each foraminifer ecogroup has a distinct thermal preference and response to the deglacial warming (Fig. 1). Both show that symbiont-barren non-spinose foraminifera keep a preference to grow in cold waters at around –1-0°C during the warming (Fig. 1). This conservative thermal preference accompanies their notable poleward displacement toward the Arctic (Fig. S2). In contrast, the other two ecogroups display a strong thermal acclimating capacity, adjusting their niche to grow in warmer waters (Fig. 1). Symbiont-barren spinose foraminifera increased their thermal optimum by about 7°C (from 5°C to 13/10°C in the model/observations; Fig. 1) allowing them to stay in the subpolar/temperate regions (Fig. S2). Symbiont-obligate spinose foraminifera show the highest acclimation capacity, increasing their thermal optimum by about 10°C (from 19/21°C to 30/29°C in the model/observations; Fig. 1) allowing them to stay in the low latitudes (Fig. S2). These results agree with previous studies that warm species' optimal niche has greater variability (*21*). Our study shows that two out of three foraminifera ecogroups acclimated to warmer temperatures during the last deglacial period.

This result could come from the fact that each ecogroup is dominated by a specific foraminifera species (*Neogloboquadrina pachyderma, Globigerina bulloides, Globigerinoides ruber albus*; Table S1). To test for species-level acclimation, we estimated the thermal performance of the top 26 foraminifera species from the fossil observations (Fig. S3). Similar to the ecogroups, we found that most species increased their thermal optimum allowing them to maintain their habitat (Fig. S4). However, species acclimated to a different degree, and the difference of species optimal temperature change is not explained by symbiont ($F_{1,26}$ = 0.434, p = 0.516) or spine trait ($F_{1,26}$ = 1.675, p = 0.207). For example, symbiont-barren non-spinose *Turborotalita quinqueloba* exhibited a 6°C shift, while *Neogloboquadrina*

pachyderma and *Neogloboquadrina incompta* in the same ecogroup show 2 °C change with overall niche generally similar. Symbiont-bearing *Globigerinoides ruber albus* and *Globoturborotalita rubescens* display the largest species-specific thermal optimum change (8 and 9 °C), while *Globigerinoides ruber ruber* only shows 4 °C change. This indicates that ecogroups are defined by species functional traits and trait variations that are more diverse than we currently have in the model. Despite this, our model captures the response of ecogroups.

Our model and fossil data present the first evidence of acclimation of planktic foraminifera to warming experienced over a long-term paleoclimate event, with thermal optimum shifts up to 10 °C. While most foraminifera showed such acclimation over the glacial-interglacial cycles, the response is highly species-dependent

Plankton thermal performance and geographical distribution in the future

Given the thermal acclimation identified in the deglacial warmings, the question arising is whether this process protects foraminifera from the threat of rapid anthropogenic warming. To answer this question, we conducted a series of transient simulations from pre-industrial to 2100, using the same model for the last deglacial warming experiment (see **Materials and Methods**). We investigated the marine ecosystem response to four warming scenarios (+1.5, 2, 3, and 4°C by 2100 relative to the 1900-1950 average; Fig. 2 and S6). The model and observation of global mean sea-surface temperature (SST) agree on that present-day (2022) is already ~0.5 °C warmer than in 1975 (Fig 2a). By 2100, such difference of will enlarge to 0.9, 1.1, 1.9, and 2.7°C under the respective four scenarios. In response to these warmings, the ocean net primary production (NPP) drops by 3.9, 5.2, 8.9, and 12.8%, respectively (Fig. 2a). Our model responses are within the Coupled Model Intercomparison Project (CMIP) range (Fig S6-7), justifying the use of our model in assessing the future foraminiferal response.

Unexpectedly, our model's future foraminifera do not acclimate as much as in the deglacial warming (Fig. 2) despite experiencing a lower warming (1-4 °C compared to 6 °C). As a result, our model predicts that the planktic foraminifera community shifts habitat towards temperate and polar regions, as already observed for the historical period (*27*). In particular, our model predicts that warm-adapted taxa (symbiont-obligate spinose) will increase biomass in the colder waters of the subantarctic zone and the North subpolar regions (Fig. 2c). The changes have already been observed in the Arctic (*28*) and cold upwelling area of the Santa Barbara Basin (*29*). Our model also predicts symbiont-barren spinose foraminifera, such as *G. bulloides*, to increase biomass in the Southern Ocean and North Atlantic (Fig. 2c). This invasion could induce new competition with local symbiont-barren non-spinoses, such as *N. pachyderma* (*30*), that has the unique ability to overwinter in sea ice (*31*). Our study thus shows that future warming will drive most planktic foraminifera to migrate poleward by 2100, contrasting with their behavior experienced during the last deglacial warming.

Along with poleward migrations, the future foraminifera limited thermal acclimation causes a biomass reduction (Fig 2a). The model estimates that global foraminifera biomass has

declined by 2.3% at the present-year (2022) relative to 1975 (Fig 2a). With a warming of 1.5, 2, 3, and 4°C by 2100, foraminifera biomass reduces further to 4.8, 6.4, 9.8% and 14.3%, respectively. This biomass loss is widespread across the ocean except in the Southern Ocean and to a lower degree in the North subpolar regions, where migration occurs (Fig. 2c). This biomass loss is uneven across ecogroups. It is primarily driven by the two symbiont-barren groups (8-24% and 8-22% for spinose and non-spinose, respectively) accounting for ~75% of the total foraminifera biomass change (between 1975 and 2100; Fig. S8). These non-symbiont groups are the most impacted probably because they are heterotrophic feeders, which rely for food only on a decreasing phytoplankton biomass. In contrast, symbiotic foraminifera are more resilient (1-10% biomass loss; Fig. S8) relying on multiple energy pathways and already adapted to a warm environment. Overall, despite observed acclimation to past warming, we found that anthropogenic warming could strongly impact planktic foraminifera, reducing their global biomass by up to 14%. This impact could be even more pronounced when considering ocean acidification's effect on calcification and symbiont bleaching , which is not included in our model.

Discussion

In contrast to previous studies suggesting conservative planktic foraminifera niche (*20*, *21*, *32*), our results reveal that that foraminifera can shift thermal niche and acclimate to the geological warming. We argue that previous studies focusing on the overall niche similarity (*20*, *21*) and occurrence data masked the change of thermal maximum or optimum (*7*, *8*). For instance, both Antell et al. (2021) and Waterson et al. (2016) used probability density function to reconstruct foraminifera niche in the glacial-interglacial cycle and calculated the similarity (overlapping). This method, however, is not sensitive enough to detect the acclimation because an idealized 1 °C shift of SST normal distribution only causes 5% overall dissimilarity (Fig. 3a). Instead, by reanalyzing the species optimal temperature obtained from Antell et al. (*20*), we find the consistently striking variation (-5 to +5°C) despite the independent methodology (Fig. 3b). Such changes of thermal optimum are also significantly correlated with regional ocean temperature ($p = 0.0086$), suggesting that foraminifera (24 species) have generally acclimated to climate change in the past 600 ka. Therefore, our finding of thermal acclimation between the LGM and the PI is replicated in the longer glacial-interglacial cycles and lends support to the late Quaternary glacial-interglacial foraminifera evolution (*33*) allowing them to persist in a dynamic climate and increase successful species evolution. The masked shifted thermal preference therefore will then introduce biases when one applies any fixed niche-based models (*34*) or modern calibrated temperature transfer function (*35*).

However, while most foraminifera acclimated during the geological warming, their thermal acclimation saturates in the modeling future. This disparity might come from the fact that the increasing ocean temperature is approaching the maximum tolerable temperatures of the current foraminifera trait set in the model. Alternatively, it can arise from the difference between the LGM equilibrium experiment and a future transient warming where changes are faster and still developing. In either way, the limited modeled foraminiferal thermal

acclimation to the rapid anthropogenic warming align with other zooplankton (copepods) in a 50-year observation (*36*), causing a foraminifera poleward shift. Observation in the Southern Ocean has already found increased foraminifera abundance by 15% during 1997-2018 (*37*). Other plankton species distribution models also predict more zooplankton in the future subpolar region (*13*). These results differ from the offline model ForamCLIM (*34*) based on a fixed growth curve which predicted increasing foraminifera abundance in the subtropics and decreasing in the subpolar regions by 2100 (*34*), highlighting the novel trait-based understanding provided in our mechanistic model. However, both models agree that foraminifera will face declining biomass (5-14% decline by 2100 relative to 1975 in our model; Fig. 2a) (*30*, *34*) as the total zooplankton community (5-15% by 2100 relative to 1990–1999 in the latest CMIP models) (*38*).

The acclimation capacity varies and depends on the functional traits. For instance, the modeled calcite spines allow spinose foraminifera to capture larger prey, causing them to rely more on food availability than temperature (Fig. S5). This result is well supported by feeding experiments (*39*) and observations in productive upwelling regions (*40*, *41*). Our study also shows that the symbiont-obligate spinose acclimate better than the other foraminifera ecogroups (Fig. 1, Fig. 2b). A likely explanation is that symbiont-obligate spinose have both autotrophic and heterotrophic energy intake, which benefit from higher temperature and light (*42*). But symbionts and spines are not the only two influencing acclimation. More functional traits exist (e.g., shell morphology, life cycle, asexual reproduction) on the species level (*22*, *23*, *43*), which might cause the diverse response to warming (Fig. S3).

Our model ignores several factors that could influence the response of foraminifera to climate changes. Firstly, foraminifera are immobile zooplankton that need to overcome dispersal problem to achieve distribution shift in real oceans. Frontal systems with abrupt environmental change and coastlines can interrupt foraminifera to migrate to a more suitable environment (*44*), and ocean currents can hinder their shifts when the current goes in the opposite direction to the temperature gradient (*45*). Such passive trait possibly causes their lower-than-average latitudinal shift rate (~40 km dec^{-1} (*27*) compared to ~100 km dec^{-1} of zooplankton mean (*6*)), and potentially inducing stronger vulnerability to warming. Besides, future ocean acidification might stress foraminifera calcification (*46*). Lower pH has already caused foraminifera shells to thin (*47*), and the risk in high latitudes will be highest due to its lowest calcite saturation state (*34*). Currently, the role of environmental factors (temperature, calcite saturation state) in influencing foraminifera calcification is not yet resolved. More studies are needed to have a comprehensive and mechanistic understanding of foraminiferal vulnerability under warming.

Assessing the species response mechanism to climate change is necessary for marine biodiversity conservation (*48*). Our trait-based foraminifera model and fossil observations provide the first long-term thermal acclimation evidence, which contrasts with the current assumption of a foraminifera conservative niche. We also found that foraminifera acclimation will be limited in the next century, which means marine plankton in the future faces non-analogue challenge. The risk to marine ecosystem is likely more complex than our estimates due to the species-level trait difference as we showed in the glacial-interglacial

experiment, and the unclear mechanism of symbiont bleaching, deoxygenation and ocean acidification, and potentially synergistic stressors.

Acknowledgments

R.Y. is funded by China Scholarship Council (202006380070) and Bob Savage Funding. R.Y. also acknowledges the Jasmin service to access CMIP data. F.M.M. thanks NERC for its funding (NE/X001261/1, NE/V01823X/1). D.N.S. was supported by NERC grant NE/P019439/1.

Data and code availability

The cGENIE model code is publicly available at https://github.com/derpycode/cgenie.muffin. Instructions including commands to run the models are included in the genie-userconfig/FORAMECOGEM/readme.md. The existing pre-industrial, LGM and Future outputs are stored in 10.5281/zenodo.8189647. Foraminifera abundance and temperature data are available at 10.5281/zenodo.8189768. CMIP6 data can be downloaded from https://esgf-node.llnl.gov/projects/cmip6/. The reanalysis of Antell et al. (2021) is available in 10.5281/zenodo.8189772.

265 .

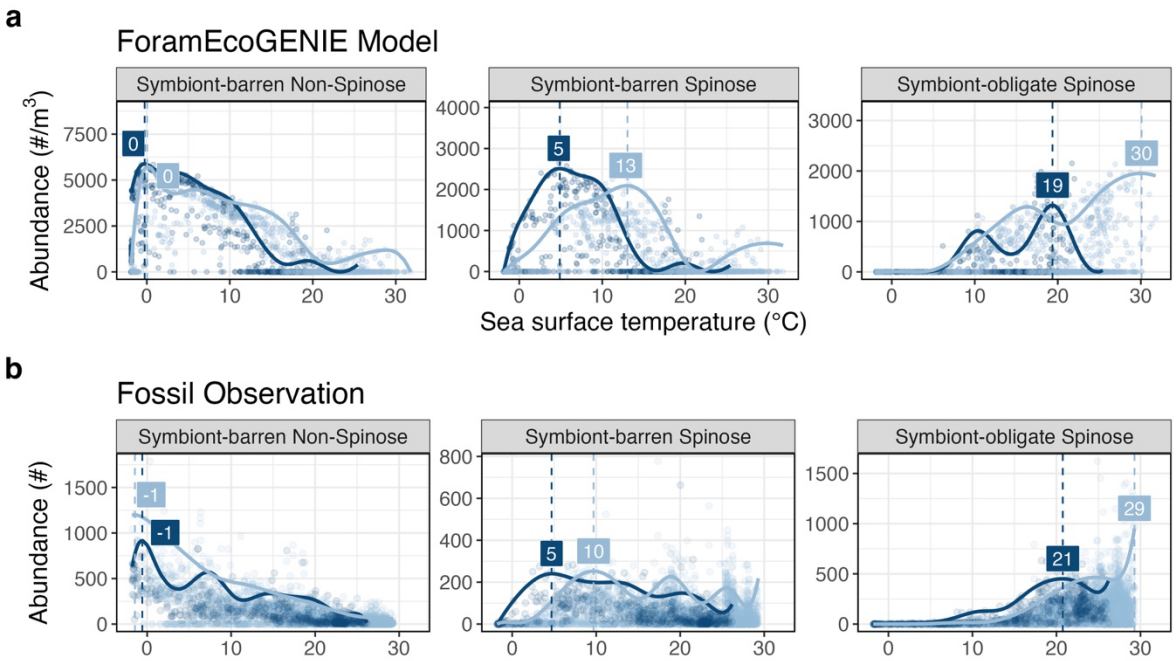

266
267 **Fig. 1. Reconstructed thermal performance of planktic foraminiferal ecogroups during the Last Glacial**
268 **Maximum (dark blue, 18-21 ka) and the pre-industrial age (light blue, 0 ka).** (a) ForamEcoGENIE model
269 output and (b) fossil records. Raw data are plotted in shaded dots. We estimated the maximum
270 thermal performance curves (continuous lines) as an unweighted 95th quantile regression following
271 Kremer et al. (2017; (*49*). We also plotted the optimal temperature (vertical dashed lines) as the best
272 temperature for species performance (abundance). The change of optimal temperature shows
273 foraminifer acclimation potential to the deglacial warming. Note the symbiont-barren spinose
274 ecogroup has more than one optimal temperature which is not labeled.

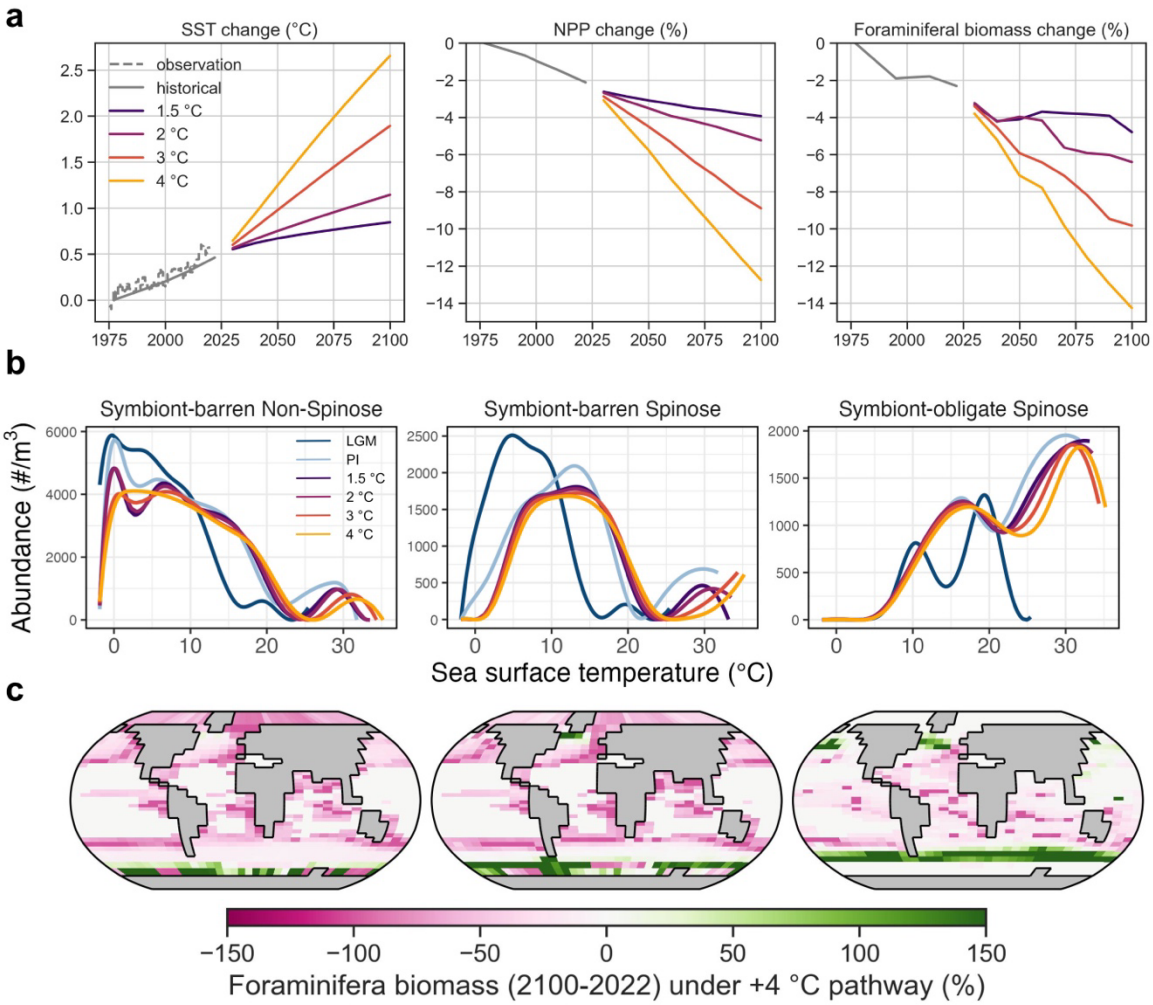

Fig. 2. Plankton ecosystem response to future anthropogenic warming in cGENIE. (a) Modeled change in sea-surface temperature, net primary production, and globally integrated foraminifera biomass when global mean surface temperature increases by 1.5, 2, 3, and 4°C by 2100 relative to the 1900-1950 average. The historical observation of SST is from ERSSTv5 (*50*). We used linear CO_2 forcings to mimic global warming. (b) Thermal performance curves of the three foraminifera ecogroups as estimated in Fig. 1 and compared to LGM and PI trends. Only the symbiont-obligate foraminifera experiences slight acclimation at 20-30 °C. (c) Biomass change of each foraminifera group under +4 °C scenario by 2100 relative to the present year (2022).

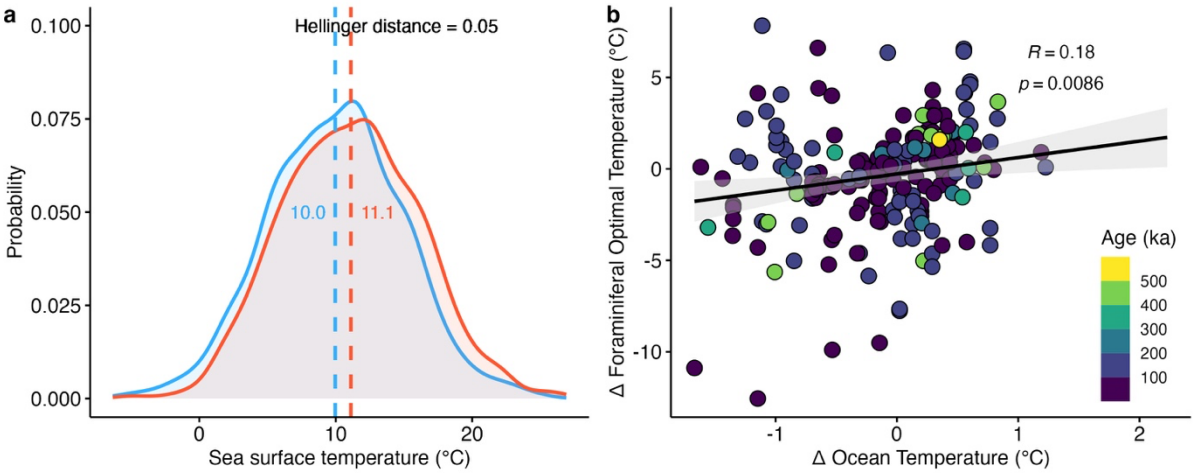

Fig. 3. Foraminiferal thermal acclimation in longer glacial-interglacial cycles (0-600 ka). (a) A schematic example of a normal distribution around 10 and 11 °C (with standard deviation of 5 °C), which shows the high similarity measured in Hellinger's distance (value range: 0 to 1, lower the more similar) used in Antell et al. (*20*) that reconstructed thermal niches change using Kernel Density Estimate (KDE) probability density distribution. (b) Based on the same data, we calculate the changes of each species' (n=24) optimal temperature (the vertical line in the left) and corresponding regional mean temperature change every 8 ka. We filter the samples with an insufficient number of occurrences (n=20) to achieve a robust reconstruction. The weak but significant relationship between ocean temperature change and species optimal temperature change indicates consistent thermal acclimation in the past 600 ka, while the rest of variance can come from uncounted climatic drivers and species-specific difference as the LGM/PI.

References

1. G. Beaugrand, A. McQuatters-Gollop, M. Edwards, E. Goberville, *Nature Climate Change*. **3**, 263–267 (2013).

2. S. Finnegan *et al.*, *Science*. **348**, 567–570 (2015).

3. M. T. Burrows *et al.*, *Science*. **334**, 652–655 (2011).

4. J. M. Sunday, A. E. Bates, N. K. Dulvy, *Nature Clim Change*. **2**, 686–690 (2012).

5. M. L. Pinsky, B. Worm, M. J. Fogarty, J. L. Sarmiento, S. A. Levin, *Science*. **341**, 1239–1242 (2013).

6. E. S. Poloczanska *et al.*, *Nature Clim Change*. **3**, 919–925 (2013).

7. C.-E. Schaum *et al.*, *Nat Ecol Evol*. **1**, 0094 (2017).

8. D. Padfield, G. Yvon-Durocher, A. Buckling, S. Jennings, G. Yvon-Durocher, *Ecology Letters*. **19**, 133–142 (2016).

9. R. F. Strzepek, P. W. Boyd, W. G. Sunda, *Proc. Natl. Acad. Sci. U.S.A.* **116**, 4388–4393 (2019).

10. A. J. Irwin, Z. V. Finkel, F. E. Müller-Karger, L. Troccoli Ghinaglia, *Proc. Natl. Acad. Sci. U.S.A.* **112**, 5762–5766 (2015).

11. Y. H. Lee *et al.*, *Nat. Clim. Chang.* **12**, 918–927 (2022).

12. G. Beaugrand, M. Edwards, V. Raybaud, E. Goberville, R. R. Kirby, *Nature Clim Change*. **5**, 695–701 (2015).

13. F. Benedetti *et al.*, *Nat Commun*. **12**, 5226 (2021).

14. X. Morin, W. Thuiller, *Ecology*. **90**, 1301–1313 (2009).

15. W. J. Chivers, A. W. Walne, G. C. Hays, *Nat Commun*. **8**, 14434 (2017).

16. B. A. Ward *et al.*, *Journal of Advances in Modeling Earth Systems*. **11**, 3343–3361 (2019).

17. CLIMAP PROJECT MEMBERS, *Science*. **191**, 1131–1137 (1976).

18. MARGO Project Members, *Nature Geosci*. **2**, 127–132 (2009).

19. G. Neukermans *et al.*, *Earth-Science Reviews*. **239**, 104359 (2023).

20. G. S. Antell, I. S. Fenton, P. J. Valdes, E. E. Saupe, *PNAS*. **118** (2021), doi:10.1073/pnas.2017105118.

21. A. M. Waterson, K. M. Edgar, D. N. Schmidt, P. J. Valdes, *Paleoceanography*. **32**, 74–89 (2017).

22. A. G. M. Caromel, D. N. Schmidt, I. Fletcher, E. J. Rayfield, *Journal of Micropalaeontology*, 2014–017 (2015).

23. C. V. Davis *et al.*, *Science Advances*. **6**, eabb8930 (2020).

24. K. Vanadzina, D. N. Schmidt, *Paleobiology*. **48**, 120–136 (2022).

25. B. A. Ward *et al.*, *Geosci. Model Dev.* **11**, 4241–4267 (2018).

26. R. Ying, F. M. Monteiro, J. D. Wilson, D. N. Schmidt, *Geoscientific Model Development*. **16**, 813–832 (2023).

27. L. Jonkers, H. Hillebrand, M. Kucera, *Nature*. **570**, 372–375 (2019).

28. M. Greco, K. Werner, K. Zamelczyk, T. L. Rasmussen, M. Kucera, *Global Change Biology*. **28**, 1798–1808 (2022).

29. D. B. Field, T. R. Baumgartner, C. D. Charles, V. Ferreira-Bartrina, M. D. Ohman, *Science*. **311**, 63–66 (2006).

30. M. Grigoratou, F. M. Monteiro, J. D. Wilson, A. Ridgwell, D. N. Schmidt, *Glob Change Biol*, in press, doi:10.1111/gcb.15964.

31. M. Greco, L. Jonkers, K. Kretschmer, J. Bijma, M. Kucera, *Biogeosciences*. **16**, 3425–3437 (2019).

32. K. M. Edgar *et al.*, *Geology*. **41**, 15–18 (2013).

33. K. F. Darling, M. Kucera, C. J. Pudsey, C. M. Wade, *Proc. Natl. Acad. Sci. U.S.A.* **101**, 7657–7662 (2004).

34. T. Roy, F. Lombard, L. Bopp, M. Gehlen, *Biogeosciences*. **12**, 2873–2889 (2015).

35. A. P. Ballantyne, M. Lavine, T. J. Crowley, J. Liu, P. B. Baker, *Geophysical Research Letters*. **32** (2005), doi:10.1029/2004GL021217.

36. S. L. Hinder *et al.*, *Global Change Biology*. **20**, 140–146 (2014).

37. M. H. Pinkerton *et al.*, *Deep Sea Research Part I: Oceanographic Research Papers*. **162**, 103303 (2020).

38. D. P. Tittensor *et al.*, *Nat. Clim. Chang.* **11**, 973–981 (2021).

39. O. R. Anderson, M. Spindler, A. W. H. Bé, Ch. Hemleben, *J. Mar. Biol. Ass.* **59**, 791–799 (1979).

40. B. J. Taylor *et al.*, *Quaternary Science Reviews*. **191**, 256–274 (2018).

41. R. Schiebel, J. Bijma, C. Hemleben, *Deep Sea Research Part I: Oceanographic Research Papers*. **44**, 1701–1713 (1997).

42. J. D. Ortiz, A. C. Mix, R. W. Collier, *Paleoceanography*. **10**, 987–1009 (1995).

43. L. Jonkers, C. E. Reynolds, J. Richey, I. R. Hall, *Biogeosciences*. **12**, 3061–3070 (2015).

44. M. T. Burrows *et al.*, *Nature*. **507**, 492–495 (2014).

45. J. García Molinos, M. T. Burrows, E. S. Poloczanska, *Sci Rep*. **7**, 1332 (2017).

46. H. Kawahata *et al.*, *Progress in Earth and Planetary Science*. **6**, 5 (2019).

47. A. D. Moy, W. R. Howard, S. G. Bray, T. W. Trull, *Nature Geoscience*. **2**, 276–280 (2009).

48. F. Seebacher, C. R. White, C. E. Franklin, *Nature Clim Change*. **5**, 61–66 (2015).

49. C. T. Kremer, M. K. Thomas, E. Litchman, *Limnology and Oceanography*. **62**, 1658–1670 (2017).

50. X. Lan, P. Tans, K. Thoning, NOAA Global Monitoring Laboratory, Trends in globally-averaged CO2 determined from NOAA Global Monitoring Laboratory measurements. (2023), , doi:10.15138/9N0H-ZH07.